*Desalination and Water Treatment*
www.deswater.com

doi: 10.5004/dwt.2021.27006

220 (2021) 232–240
April

# Design and preparation of novel functional resin D301-*g*-polyvinylimidazole for recovering Au(III) from aqueous solution

Feng Gao, Wen-Hua Gao, Xiao-Qin Feng, Tuo-Ping Hu, Jian-Feng Gao, Fu-Qiang An*

*Chemical Department, North University of China, Taiyuan 030051, China, Tel. 86-351-3923197; emails: anfuqiang@nuc.edu.cn (F.-Q. An), 18404905595@163.com (F. Gao), 2281602484@qq.com (W.-H. Gao), 995502673@qq.com (X.-Q. Feng), tuopinghu@126.com (T.-P. Hu), gaojianfeng@163.com (J.-F. Gao)*

Received 4 August 2020; Accepted 4 Janaury 2021

**ABSTRACT**

Resin adsorbent for gold recovery have the characteristics of simple preparation, good reusability and low consumption performance, but their shortcomings of low adsorption efficiency and poor adsorption capacity cannot be ignored. Based on this, a novel adsorbent with high adsorption performance towards Au(III) was prepared by functionalizing D301 resin with 1-vinylimidazole using the surface-initiated graft-polymerization method. The physicochemical characteristics of D301-*g*-PVIM (PVIM – polyvinylimidazole) were characterized by Fourier-transform infrared spectroscopy, scanning electron microscopy, Brunauer–Emmett–Teller and elemental analysis. The adsorption capacity of Au(III) was studied by a static adsorption experiment. The maximum adsorption capacity of D301-*g*-PVIM for Au(III) was 543.9 mg $g^{-1}$. The kinetic study shows that the adsorption data can well described by the pseudo-second-order kinetic model. The equilibrium isotherm for the adsorption of Au(III) on D301-*g*-PVIM has a good correlation with the Freundlich model, and the adsorption is a multilayer sorption. The adsorption thermodynamics study indicated that the adsorption process is spontaneously endothermic. Repeated use experiments showed that D301-*g*-PVIM has high efficiency and good regeneration performance.

*Keywords:* Adsorption; Au(III); 1-Vinylimidazole; Graft polymerization; D301

## 1. Introduction

Gold has a wide range of applications in various fields because of its good physical and chemical properties [1,2]. At the same time, the growing industry's demand for precious metals has made rare metal resources increasingly scarce. Therefore, the recovery of gold is of great significance. Various approaches including ion exchange, extraction, chemical precipitation and adsorption have been used for recovering gold from wastewater [3–5]. In the above methods, adsorption is considered to be the most promising approach due to its low cost, good separation effect, and high flexibility [6]. Compared with activated carbons, silica, clay and other inorganic adsorbents, the adsorption resins have higher adsorption efficiency due to the coordination interaction between functional groups and metals [7–10]. For adsorption resins, the adsorption capacity largely depends on the number and type of functional groups such as –N, O, S and other functional groups, which can form a strong binding ability with metal ions [11,12]. Therefore, it is very important to improve the adsorption efficiency of the resin by introducing special functional groups.

D301 is a kind of weakly basic ion exchange material with a porous structure, which is widely used in the adsorption of heavy metals [13]. Some research have demonstrated the modification of weakly basic resin D301

* Corresponding author.

to improve its adsorption capacity and selectivity, such as ethylenediamine thiourea, poly-epichlorohydrin-dimethylamine, 2-aminopyridine to adsorb $AuCl_4^-$, Cr(VI), glyphosate [12,14,15]. Graft polymerization is widely used to prepare adsorbents with special functional groups [16]. In this way, the properties of different substrates can be modified to adsorb different target ions [17]. 1-Vinylimidazole (VIM) has a special chelating effect on metal ions due to its imidazole ring. The research on the use of VIM to remove heavy metals has been reported. For example, polyvinylimidazole (PVIM) modified cellulose was used to remove Cr(VI), the maximum adsorption capacity reached 134 mg $g^{-1}$ [18]. Silica-graft-vinyl imidazole were applied for Hg(II) removal [19]. However, to our knowledge, there have never been reported about VIM graft resins for gold recovery. According to Pearson's HSAB theory [20], Au is classified as a soft acid, which can be chelated with the N atom that belonging to the soft base. There are two N atoms in a VIM molecule, the adsorbent functionalized with VIM is expected to be useful for the removal of Au(III) from wastewater.

In this study, the grafted material D301-*g*-PVIM was prepared by using the graft polymerization method. The D301-*g*-PVIM was characterized by scanning electron microscopy (SEM), Fourier-transform infrared spectroscopy (FTIR), specific surface area analysis ($S_{BET}$) and elemental analysis. The adsorption capacity of D301-*g*-PVIM towards Au(III), adsorption thermodynamics and adsorption kinetics were studied through batch adsorption experiments.

## 2. Experimental

### 2.1. Materials and instruments

D301 resin was purchased from Wandong Chemical Co., Ltd., (Anhui, China). 1-Vinylimidazole (VIM) was purchased from Jin Sheng Ji Chemical Co., Ltd., (Guangdong, China). Chloroauric acid was obtained from Nanjing Chemical Reagent Co., Ltd., ($HAuCl_4$, Nanjing, China, AR grade). Ammonium persulfate (APS) was supplied by Kay Tong Chemical Reagent Co., Ltd., (Tianjin, China, AR grade), thiourea, hydrochloric acid and other reagents were purchased from Beijing Chemical Plant (Beijing, China, AR grade).

Instruments used in this study are as follows: Prodigy Inductively Coupled Plasma-Atomic Emission Spectrometry (ICP-AES) (Leeman Labs, America), FTIR-8400S infrared spectrometer (Shimadzu, Japan), Autosorb-iQ surface area analyzer (America), Vario EL elemental analyzer (Elementar, Germany), SU8220 scanning electron microscope (Hitachi Company, Japan), PHS-3 acidimeter (Shanghai INESA Scientific Instrument Co., Ltd., China), SHZ-C water-bathing constant temperature shaker (Shanghai Boxun Medical Biological Instrument Co., Ltd., China).

### 2.2. Preparation and characterizations of D301-*g*-PVIM

The synthesis route of the D301-*g*-PVIM is shown in Fig. 1. 1 g of particles D301 and 8 mL of 1-vinylimidazole were added into 40 mL of dimethylformamide, then graft polymerization was performed by initiating ammonium persulfate (APS) (1.4 wt.% of monomer) under $N_2$ atmosphere at 40°C for 10 h. After the reaction, the resin was repeatedly washed with ethanol and distilled water to remove the polymer that adsorbed on the surface of the particles, and then dried in a vacuum. The grafted material D301-*g*-PVIM was obtained.

The specific surface area ($S_{BET}$) of D301-*g*-PVIM was measured using the $N_2$ adsorption–desorption method, the total pore volume was calculated from the liquid volume of nitrogen at a relative pressure ($p/p_0$) of 0.99. The surface morphology of D301 and D301-*g*-PVIM were characterized by a scanning electron microscope. FTIR spectra was performed using the traditional KBr pellet technique. The element content was measured by the elemental analyzer.

### 2.3. Adsorption experiments

The batch adsorption method was used to carry out the adsorption experiment. 10 mg of the D301-*g*-PVIM and 200 mL of 30 mg $L^{-1}$ Au(III) solution are mixed and shaken in a water-bathing constant temperature shaker, and the concentration of Au(III) was measured by ICP at different times. The influences of contact time, initial Au(III) concentration, solution pH value, temperature, and the dosage of adsorbent on adsorption abilities were investigated. The adsorption capacity was calculated by Eq. (1). The adsorption efficiency $A_f$ was calculated by Eq. (2).

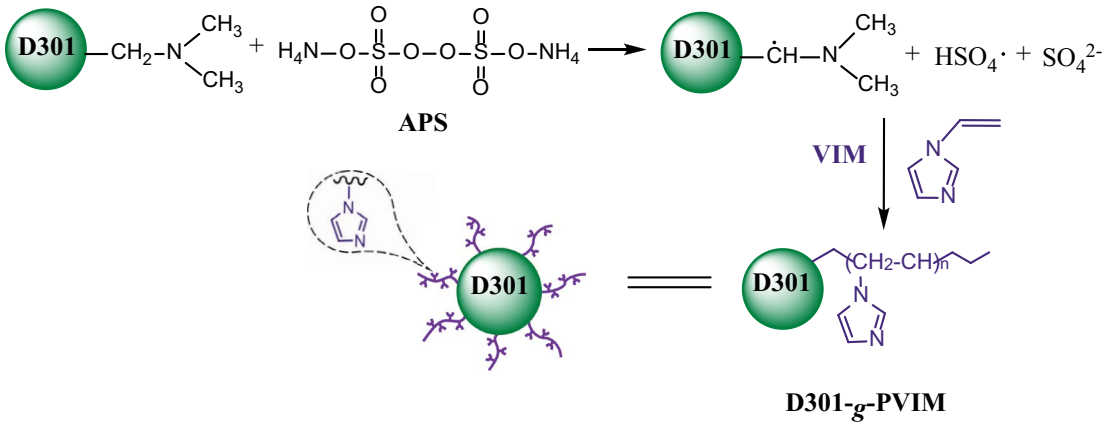


Fig. 1. Synthesis route of D301-*g*-PVIM.

$$Q_e = \frac{(C_0 - C_t)V}{m} \quad (1)$$

$$A_f = \frac{C_0 - C_t}{C_0} \times 100\% \quad (2)$$

where $Q_e$ is the adsorption capacity (mg g$^{-1}$), $C_0$ and $C_t$ are the initial concentration and $t$ time concentration in the solution (mg L$^{-1}$), $V$ is the volume of the solution (L), and $m$ is the mass (g) of D301-*g*-PVIM.

### 2.4. Repeated use experiment

Reusability is an important factor to testing the adsorbent for practical usage. Thiourea is usually used as the eluent for leaching gold because of its strong binding ability to gold [21]. The exhausted D301-*g*-PVIM was added to the 100 mL of 0.1 g L$^{-1}$ thiourea aqueous solution and stirred for 1 h to ensure the desorption of Au(III) from the adsorbent, then repeatedly washed with distilled water and dried in vacuum drying oven to regenerate the adsorbent. The adsorption–desorption process was repeated 5 times.

## 3. Results and discussion

### 3.1. Adsorbent characterization

The specific surface area $S_{BET}$ and pore size distribution of D301 and D301-*g*-PVIM are shown in Table 1. It can be seen that compared with D301, D301-*g*-PVIM has a relatively smaller pore size, larger pore-volume and specific surface area. The results show that due to the existence of these macropores on D301, VIM could be easily grafted on the surface of D301 and the grafting efficiency has also been improved. The grafting of VIM on the surface of D301 could be proved by the increase of $S_{BET}$ and pore volume. Infrared spectrum of D301 and D301-*g*-PVIM are shown in Fig. 2. It can be seen that the new absorption peaks at 1,384 and 1,108 cm$^{-1}$ belong to the characteristic absorption peaks of the imidazole ring [22,23]. The N–H stretching vibration absorption peak is obviously enhanced at 3,400 cm$^{-1}$. Combining with the elemental analysis results (Table 2) that the D301-*g*-PVIM has a higher nitrogen content than that of the D301, indicating that the surface amino groups of D301 have reacted with VIM. It shows that VIM has been successfully grafted onto D301. Gold can be effectively adsorbed by D301-*g*-PVIM through the coordination interaction between N atom and Au(III) ion.

### 3.2. SEM analysis

Fig. 3 represents the SEM images of D301 and D301-*g*-VIM, respectively. It can be found that the surface morphology of D301 resin was very smooth before VIM grafting. After grafting, the surface of D301-*g*-VIM resin became rough, which was attributed to the grafted of PVIM on the surface of D301 resin.

### 3.3. Adsorption kinetics

The kinetic adsorption curves of D301 and D301-*g*-PVIM towards Au(III) are shown in Fig. 4. The adsorption capacity of D301-*g*-PVIM is 478 mg g$^{-1}$. Compared with D301, the adsorption capacity of D301-*g*-PVIM is much improved.

The Lagergren-first-order model Eq. (3) and pseudo-second-order model Eq. (4) were used to test experimental data and describe the behavior of adsorption on Au(III). The equations are as follows:

$$\ln(Q_e - Q_t) = \ln Q_e - k_1 t \quad (3)$$

$$\frac{t}{Q_t} = \frac{1}{k_2 Q_e^2} + \frac{t}{Q_e} \quad (4)$$

where $Q_t$ (mg g$^{-1}$) is the adsorption capacity at time t (min$^{-1}$), $Q_e$ (mg g$^{-1}$) is the calculated equilibrium adsorption capacity, and $k_1$ (min$^{-1}$) and $k_2$ (g mg$^{-1}$ min$^{-1}$) are the adsorption rate constant. The linear fitting and kinetic

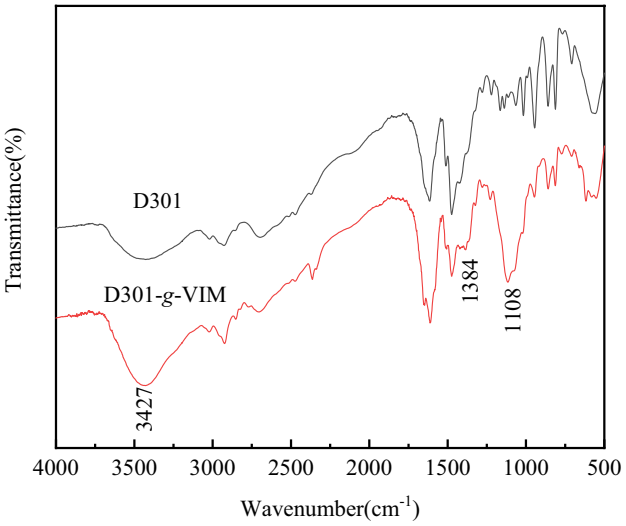


Fig. 2. FTIR spectra of D301 and D301-*g*-PVIM.

Table 1
Pore structure parameters

| Samples | $S_{BET}$ (m$^2$ g$^{-1}$) | Pore volume (cm$^3$ g$^{-1}$) | Pore size (nm) |
|---|---|---|---|
| D301 | 26.09 | 0.189 | 290.88 |
| D301-*g*-PVIM | 57.56 | 0.236 | 163.70 |

Table 2
Element analysis results

| Samples | C% | N% | H% |
|---|---|---|---|
| D301 | 58.22 | 5.97 | 7.41 |
| D301-*g*-PVIM | 61.50 | 6.41 | 7.48 |

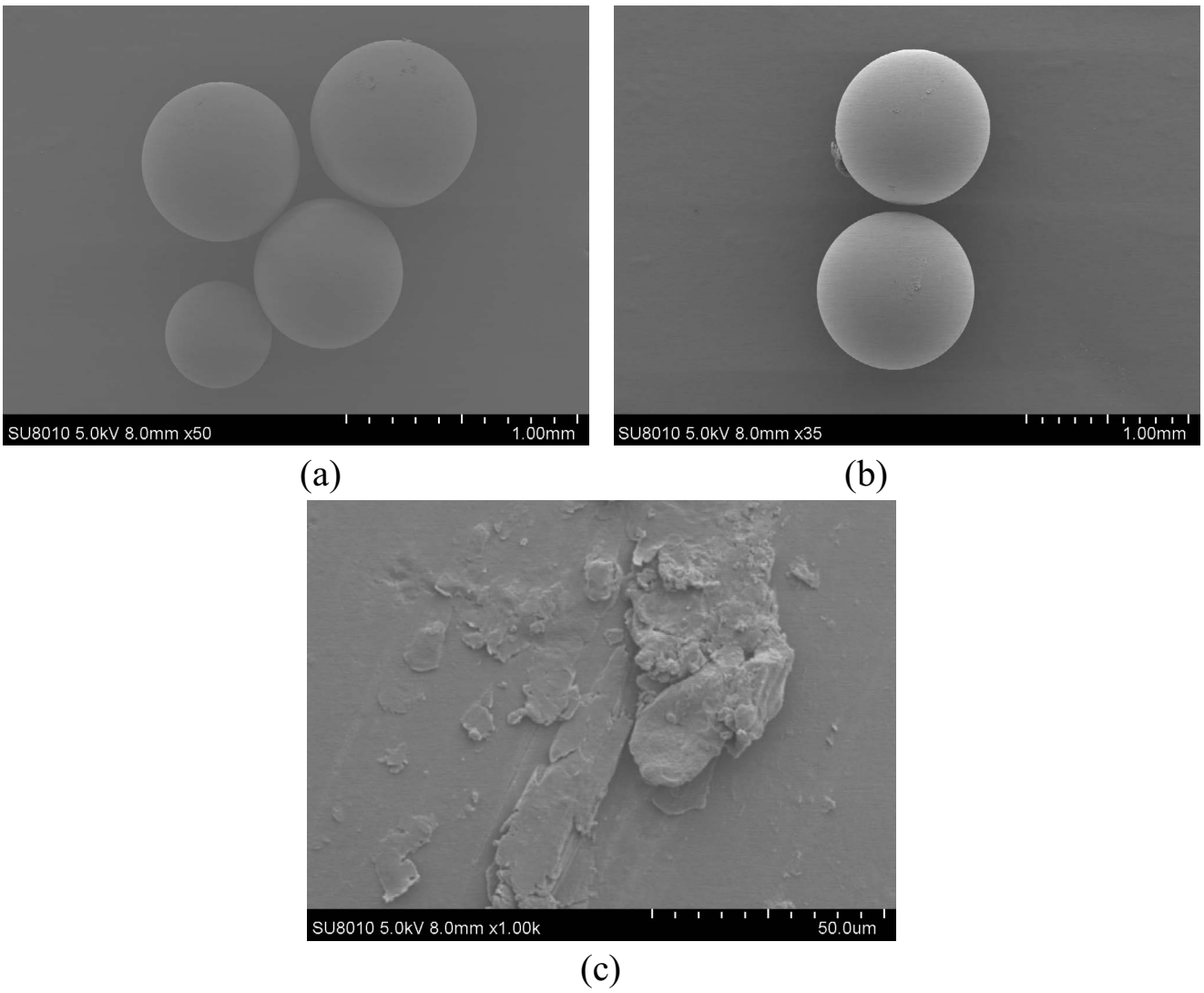


Fig. 3. SEM images of D301 (a) and D301-*g*-PVIM (b and c).

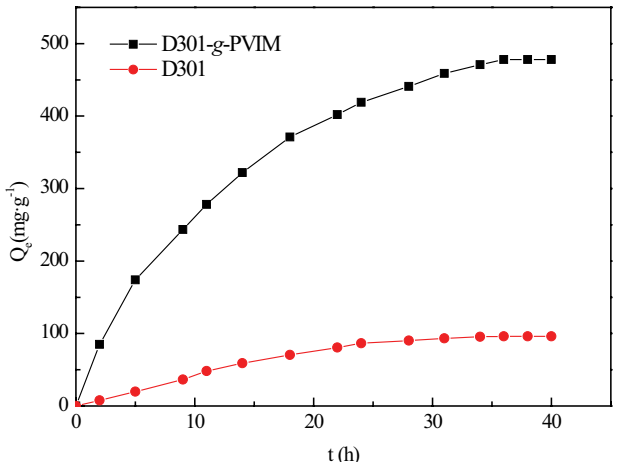


Fig. 4. Adsorption kinetics of Au(III) curves pH = 2; $T$ = 298 K; adsorbent dosage, 0.01 g; initial concentration, 30 mg $L^{-1}$.

parameters of the two models were shown in Fig. 5 and Table 3, respectively.

It is obvious from Fig. 5 that the correlation coefficient ($R^2$) value of the pseudo-second-order is larger than that of the Lagergren-first-order and the experimental data is more consistent with the pseudo-second-order kinetic model. The pseudo-second-order model is more suitable for describing the adsorption process. The reason can be interpreted as chemisorption is a rate control step and it depends on the number of surface adsorption site [24,25]. The adsorption mechanism could be explained as metal ion chelation between imidazole ring and gold ion. Because the N atoms in the imidazole ring, which is regarded as a soft base, have a strong binding ability to the Au(III), which is regarded as a soft acid according to Pearson HSAB theory [20].

Table 4 shows the comparison of Au(III) adsorption capacity with other adsorbents, it can be seen that D301-*g*-PVIM showed a good adsorption ability.

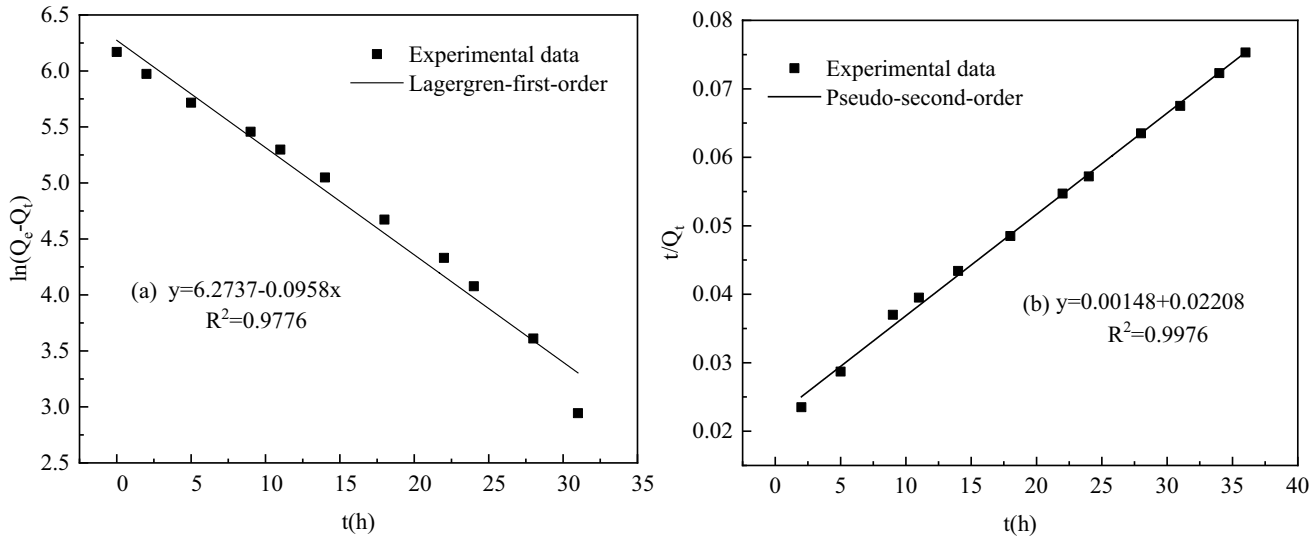


Fig. 5. Linear fitting of Lagergren-first-order (a) and pseudo-second-order (b).

Table 3
Fitting results of dynamic equations

| Lagergren-first-order | | | Pseudo-second-order | | |
|---|---|---|---|---|---|
| $Q_e$ (mg g$^{-1}$) | $k_1$ (min$^{-1}$) | $R^2$ | $Q_e$ (mg g$^{-1}$) | $k_2$ (g mg$^{-1}$ min$^{-1}$) | $R^2$ |
| 530.4 | 0.0958 | 0.9776 | 675.6 | $9.94 \times 10^{-5}$ | 0.9976 |

Table 4
Comparison of adsorption capacity with other adsorbents

| Number | Adsorbents | $Q_e$ (mg g$^{-1}$) | Adsorption condition pH/T (°C) | References |
|---|---|---|---|---|
| 1 | MFT resin | 48.0 | 2/25 | [27] |
| 2 | O-MWCNTs | 62.3 | 2/25 | [28] |
| 3 | UF resin | 29.6 | 2/– | [29] |
| 4 | $Fe_3O_4$@$SiO_2$ | 115 | 3/– | [30] |
| 5 | RDPs | 78 | –/25 | [31] |
| 6 | LMCCR | 74.3 | 2/– | [32] |
| 7 | D301-*g*-PVIM | 543.9 | 2/25 | This study |

MFT: melamine-formaldehyde-thiourea; O-MWCNTs: oxidized multi-walled carbon nanotubes; UF: urea-formaldehyde; RDPs: raw date pits; LMCCR: l-lysine modified crosslinked chitosan.

### *3.4. Adsorption isotherms*

The isotherm adsorption experiments were carried out at the initial concentration of Au(III) of 5, 10, 15, 20, 25, 30 mg L$^{-1}$, respectively. The adsorption isotherm of D301-*g*-PVIM towards Au(III) is shown in Fig. 6. In order to further evaluate the adsorption process, the adsorption isotherm was analyzed by the Langmuir model Eq. (5) and Freundlich model Eq. (6). The parameters are shown in Table 5.

$$Q_e = \frac{Q_0 K C_e}{1 + K C_e} \tag{5}$$

$$Q_e = k C_e^{1/n} \tag{6}$$

where $Q_e$ (mg g$^{-1}$) is the equilibrium adsorption capacity, $Q_0$ (mg g$^{-1}$) is the monolayer adsorption capacity, $C_e$ (mg L$^{-1}$) is the equilibrium concentration, $K$ (L mg$^{-1}$) is the Langmuir constant, $k$ and $n$ are the Freundlich constant.

It can be seen from Fig. 6, the adsorption capacity of Au(III) was significantly increased with the increase of Au(III) concentration at low concentration region. In Table 5, the maximum adsorption capacity of Au(III) calculated by Langmuir model was 543.9 mg g$^{-1}$. Compared with the Langmuir model, the $R^2$ of the Freundlich model

Table 5
Fitting parameters and correlation coefficients of Langmuir and Freundlich

| Langmuir model | | | Freundlich model | | |
|---|---|---|---|---|---|
| $K$ (L mg$^{-1}$) | $Q_0$ (mg g$^{-1}$) | $R^2$ | $k$ | $n$ | $R^2$ |
| 0.393 | 543.9 | 0.9793 | 171.03 | 2.38 | 0.9941 |

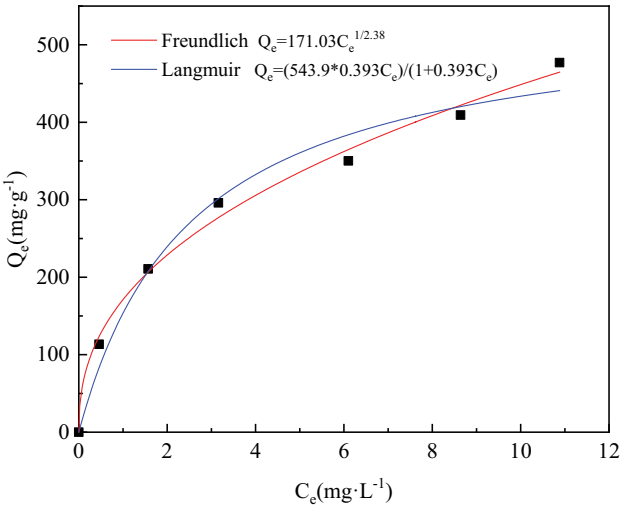


Fig. 6. Adsorption isotherm pH = 2; $T$ = 298 K; adsorbent dosage, 0.01 g; initial concentration, 5, 10, 15, 20, 25 and 30 mg L$^{-1}$.

has higher coefficient value (0.9941), which means that the adsorption process belongs to Freundlich multilayer adsorption resulting from heterogeneous distribution of VIM on the surface. Additionally, the $k$ and $n$ value represent the adsorption strength and affinity of the adsorbent for metal ions [26], the value of $1/n$ in Freundlich model is between 0.1 and 0.5, which indicates that the adsorption process of the D301-*g*-PVIM towards Au(III) is easy to carry out.

### 3.5. Effect of different pH on adsorption capacity

Fig. 7 shows the adsorption capacity of D301-*g*-PVIM towards Au(III) at different pH values.

It is worth noting that when the pH value in the solution is less than 3, the main existence form of Au(III) is $AuCl_4^-$, which can exist stably without precipitation [33]. The adsorption experiment was conducted at the initial pH of 1.0, 2.0, 3.0, respectively. The pH of the solution was adjusted by 12 M of hydrochloric acid. As shown in Fig. 7, the D301-*g*-PVIM has the best adsorption performance at pH 2. Under low pH conditions, the adsorption mechanism is mainly manifested by the protonation of N atoms on the imidazole ring, which produces electrostatic interaction with $AuCl_4^-$ [34]. When the pH value of the solution is less than 2, the surface adsorption sites are occupied by a higher concentration of chloride ions (derived from HCl used to adjust the pH), which will result in competitive adsorption with Au(III) ion. The following experiments were conducted under the condition of pH 2.

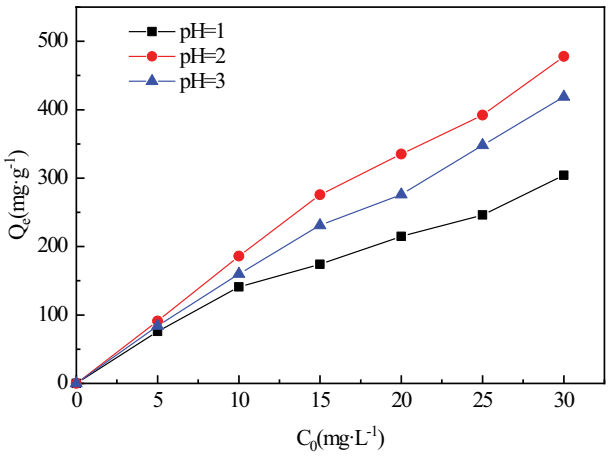


Fig. 7. Adsorption capacity in different pH $T$ = 298 K; adsorbent dosage, 0.01 g; initial concentration, 5, 10, 15, 20, 25 and 30 mg L$^{-1}$.

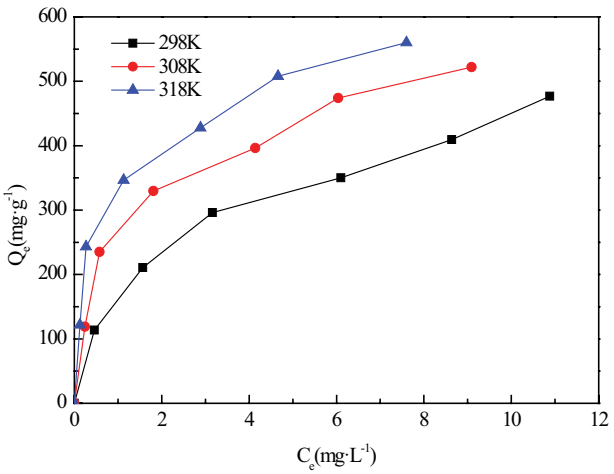


Fig. 8. Isotherms in different temperature pH = 2; adsorbent dosage, 0.01 g; initial concentration, 5, 10, 15, 20, 25 and 30 mg L$^{-1}$.

### 3.6. Thermodynamic analysis

In order to determine the influence of temperature on the adsorption ability, adsorption experiments at different temperatures were also carried out. The adsorption isotherms at different temperatures are shown in Fig. 8.

With the temperature increased, the adsorption capacity of D301-*g*-PVIM is enhanced greatly. In order to evaluate the adsorption of Au(III) thermodynamic property. The thermodynamic functions are as follows.

$$K_c = \frac{Q_e}{C_e} \tag{7}$$

$$\Delta G = -RT\ln K_c \tag{8}$$

$$\ln K_c = \frac{\Delta S}{R} - \frac{\Delta H}{RT} \tag{9}$$

where $K_c$ is the equilibrium constant, $C_e$ (mg $L^{-1}$) is the equilibrium concentration of Au(III) in the solution, $Q_e$ (mg $L^{-1}$) is the equilibrium adsorption capacity, $\Delta G$, $\Delta H$ and $\Delta S$ are the Gibbs free energy changes, enthalpy changes, entropy changes, respectively, $R$ is the universal gas constant (8.314 J $mol^{-1}$ $K^{-1}$) and $T$ (K) is the temperature.

$\Delta H$ and $\Delta S$ were calculated by the Van't Hoff linear plot ($\ln K_c$ – $1/T$) (Fig. 9) [35]. All the thermodynamic parameters are listed in Table 6.

As presented in Table 6, negative $\Delta G$ and positive $\Delta H$ reveals that the process of adsorption was a spontaneously endothermic reaction, and positive $\Delta S$ implies that the process is an entropy increasing process, which suggested that the chemical structure of D301-*g*-PVIM were considerable alternations upon interaction with Au(III). Furthermore, $\Delta G$ becomes more and more negative as the temperature increases, indicating that the temperature increase is beneficial to the reaction process, which is advantages for increasing the adsorption capacity of Au(III).

### 3.7. Influence of adsorbent dosage on the adsorption efficiency

The influence of adsorbent dosage on the adsorption capacity and adsorption efficiency are shown in Fig. 10.

It can be seen that the maximum adsorption efficiency is 99.45% at the D301-*g*-PVIM dosage of 0.045 g. Obviously, the adsorption efficiency increases along with the increase of dosage of adsorbent. The observation could be illustrated by that the number of available adsorption sites can be increased by increasing of the dosage of adsorbents, resulting the increase of the adsorption efficiency. However, when all the amount of Au(III) in the aqueous solutions were adsorbed by the adsorbents, the number of available adsorption sites still grew, which would no longer contribute to the adsorption efficiency, resulting in a decrease of adsorption capacity. It indicates that D301-*g*-PVIM can be used to recovery Au(III) in aqueous solution effectively.

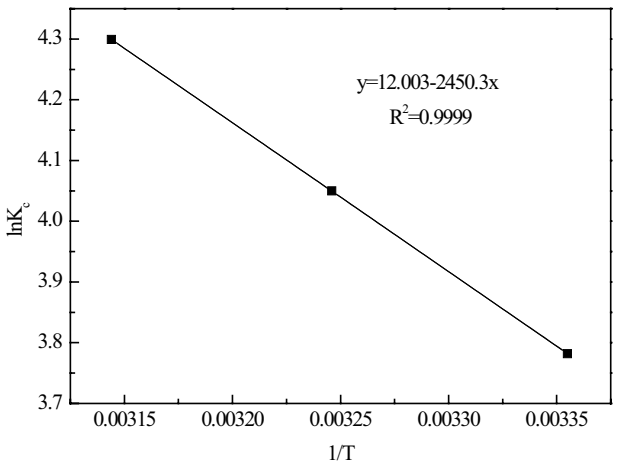


Fig. 9. $\ln K_c$ – $1/T$ fitting curve.

Table 6
Thermodynamic parameters of D301-*g*-PVIM

| $\Delta G$ (kJ $mol^{-1}$) | | | $\Delta H$ (kJ $mol^{-1}$) | $\Delta S$ (J $mol^{-1}$ $K^{-1}$) |
|---|---|---|---|---|
| 298 K | 308 K | 318 K | | |
| –9.37 | –10.37 | –11.36 | 20.37 | 99.79 |

### 3.8. Adsorbent reusability

The desorption and regeneration of adsorbent is a very important issue, especially from the perspective of practical application. The adsorption–desorption result is presented in Fig. 11.

The result clearly shows that the exhausted D301-*g*-PVIM could be effectively regenerated in 1 g $L^{-1}$ of thiourea aqueous solution. After the third time adsorption-desorption cycle, the adsorption capacity towards Au(III) basically remains unchanged. This indicates that as-prepared D301-*g*-PVIM in this work has good regeneration performance.

## 4. Conclusion

In this study, a novel grafted material D301-*g*-PVIM was prepared by polymerization using 1-vinylimidazole as monomer. The maximum adsorption capacity of Au(III) can reach 543.9 mg $g^{-1}$ and the adsorption capacity is largely depends on the pH and temperature in the solution. The adsorption process could be well described by the pseudo-second-order model and Freundlich isotherm model. Adsorption thermodynamics shows that the adsorption process can be carried out by chemical adsorption, and negative $\Delta G$ and positive $\Delta H$ indicates that the adsorption process is spontaneously endothermic. Additionally, the D301-*g*-PVIM has good reusability and regeneration performance. According to the research results, the novel grafted material D301-*g*-PVIM shows a promising application in recovering Au(III) from wastewater.

## Acknowledgments

This work was supported by the National Natural Science Foundation of China (21676258), Natural Science Foundation of Shanxi Province (201803D31061), and the

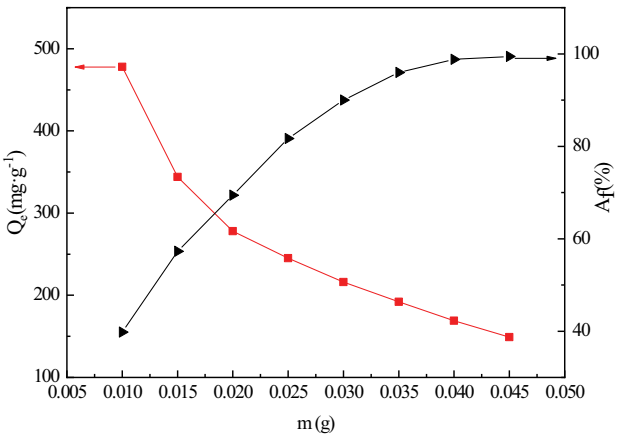


Fig. 10. Influence of adsorbent dosage on the adsorption efficiency pH = 2; $T$ = 298 K; initial concentration, 30 mg $L^{-1}$.

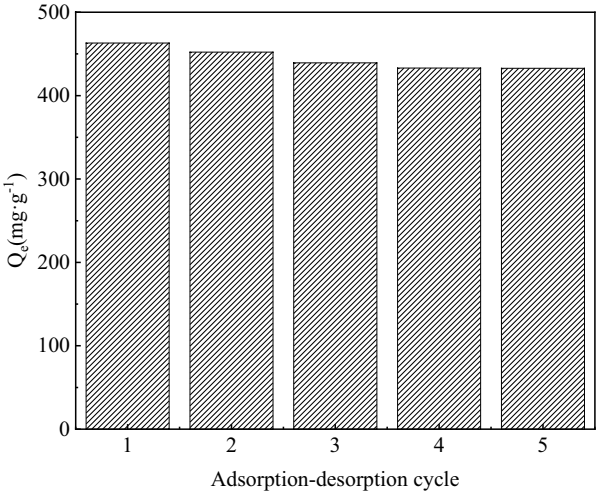


Fig. 11. Adsorption–desorption cycle of D301-*g*-PVIM.

International Scientific and Technological Cooperation Projects of Shanxi Province (201803D421080).

## References


[1] S. Kim, S. Park, S. Han, Y. Han, J. Park, Silanol-rich ordered mesoporous silica modified thiol group for enhanced recovery performance of Au(III) in acidic leachate solution, Chem. Eng. J., 351 (2018) 1027–1037.

[2] S. Syed, Recovery of gold from secondary sources—a review, Hydrometallurgy, 115 (2012) 30–51.

[3] M. Behbahani, F. Najafi, M.M. Amini, O. Sadeghi, A. Bagheri, P.G. Hassanlou, Solid phase extraction using nanoporous MCM-41 modified with 3,4-dihydroxybenzaldehyde for simultaneous preconcentration and removal of gold(III), palladium(II), copper(II) and silver(I), J. Ind. Eng. Chem., 20 (2014) 2248–2255.

[4] V.T. Nguyen, J.C. Lee, J. Jeong, B.S. Kim, G. Cote, A. Chagnes, Extraction of gold(III) from acidic chloride media using phosphonium-based ionic liquid as an anion exchanger, Ind. Eng. Chem. Res., 54 (2015) 1350–1358.

[5] I.S. Kwak, M.A. Bae, S.W. Won, J. Mao, K. Sneha, J. Park, M. Sathishkumar, Y.S. Yun, Sequential process of sorption and incineration for recovery of gold from cyanide solutions: comparison of ion exchange resin, activated carbon and biosorbent, Chem. Eng. J., 165 (2010) 440–446.

[6] F.L. Liu, S.Y. Wang, S.X. Chen, Adsorption behavior of Au(III) and Pd(II) on persimmon tannin functionalized viscose fiber and the mechanism, Int. J. Biol. Macromol., 152 (2020) 1242–1251.

[7] F.J. Cao, C. Lian, J.G. Yu, H.J. Yang, S. Lin, Study on the adsorption performance and competitive mechanism for heavy metal contaminants removal using novel multi-pore activated carbons derived from recyclable long-root *Eichhornia crassipes*, Bioresour. Technol., 276 (2019) 211–218.

[8] E. Da'na, Adsorption of heavy metals on functionalized-mesoporous silica: a review, Microporous Mesoporous Mater., 247 (2017) 145–157.

[9] M.K. Uddin, A review on the adsorption of heavy metals by clay minerals, with special focus on the past decade, Chem. Eng. J., 308 (2017) 438–462.

[10] M.A. Lira, R. Navarro, I. Saucedo, M. Martinez, E. Guibal, Influence of the textural characteristics of the support on Au(III) sorption from HCl solutions using Cyphos IL101-impregnated Amberlite resins, Chem. Eng. J., 302 (2016) 426–436.

[11] M. Pilsniak-Rabiega, A.W. Trochimczuk, Selective recovery of gold on functionalized resins, Hydrometallurgy, 146 (2014) 111–118.

[12] F.Q. An, M. Li, R.Y. Wu, T.P. Hu, J.F. Gao, Z.G. Yuan, Effective recovery of $AuCl_4^-$ using D301 resin functionalized with ethylenediamine and thiourea, Hydrometallurgy, 169 (2017) 356–361.

[13] F.Q. An, R.Y. Wu, M. Li, T.P. Hu, J.F. Gao, Z.G. Yuan, Adsorption of heavy metal ions by iminodiacetic acid functionalized D301 resin: kinetics, isotherms and thermodynamics, React. Funct. Polym., 118 (2017) 42–50.

[14] Y. Zang, Q. Yue, Y. Kan, L. Zhang, B. Gao, Research on adsorption of Cr(VI) by poly-epichlorohydrin-dimethylamine (EPIDMA) modified weakly basic anion exchange resin D301, Ecotoxicol. Environ. Saf., 161 (2018) 467–473.

[15] G. Xiao, R. Wen, Comparative adsorption of glyphosate from aqueous solution by 2-aminopyridine modified polystyrene resin, D301 resin and 330 resin: influencing factors, salinity resistance and mechanism, Fluid Phase Equilib., 411 (2016) 1–6.

[16] M.K. Song, B.T. Lee, Synthesis of $CH_3I$-quaternized polypropylene nonwoven fiber grafted with imidazole (PP-*g*-Vim) to adsorb vapor phase ammonia, Chemosphere, 233 (2019) 660–666.

[17] H. Mittal, R. Jindal, B.S. Kaith, A. Maity, S.S. Ray, Flocculation and adsorption properties of biodegradable gum-ghatti-grafted poly(acrylamide-co-methacrylic acid) hydrogels, Carbohydr. Polym., 115 (2015) 617–628.

[18] X. Peng, Z.C. Yan, L.H. Hu, R.Z. Zhang, S.J. Liu, A.L. Wang, X.W. Yu, L. Chen, Adsorption behavior of hexavalent chromium in aqueous solution by polyvinylimidazole modified cellulose, Int. J. Biol. Macromol., 155 (2020) 1184–1193.

[19] J. Sun, Z.M. Chen, M.Y. Ge, L. Xu, M.L. Zhai, Selective adsorption of Hg(II) by γ-radiation synthesized silica-graft-vinyl imidazole adsorbent, J. Hazard. Mater., 244 (2013) 94–101.

[20] R.G. Pearson, Hard and soft acids and bases, J. Am. Chem. Soc., 85 (1963) 3533–3539.

[21] A.M. Donia, A.M. Yousif, A.A. Atia, M.F. Elsamalehy, Efficient adsorption of Ag(I) and Au(III) on modified magnetic chitosan with amine functionalities, Desal. Water Treat., 52 (2014) 2537–2547.

[22] L.S. Shao, J.H. Huang, Controllable synthesis of N-vinylimidazole-modified hyper-cross-linked resins and their efficient adsorption of p-nitrophenol and o-nitrophenol, J. Colloid Interface Sci., 507 (2017) 42–50.

[23] C.R.T. Tarley, M.Z. Corazza, B.F. Somera, M.G. Segatelli, Preparation of new ion-selective cross-linked poly(vinylimidazole-co-ethylene glycol dimethacrylate) using a double-imprinting process for the preconcentration of $Pb^{2+}$ ions, J. Colloid Interface Sci., 450 (2015) 254–263.

[24] R.J. Huang, N. Shao, L. Hou, X.L. Zhu, Fabrication of an efficient surface ion-imprinted polymer based on sandwich-like graphene oxide composite materials for fast and selective removal of lead ions, Colloids Surf., A, 566 (2019) 218–228.

[25] X.L. Wu, Y.L. Wu, H.J. Dong, J. Zhao, C. Wang, S. Zhou, J. Lu, Y.S. Yan, H. Li, Accelerating the design of molecularly imprinted nanocomposite membranes modified by Au@polyaniline for selective enrichment and separation of ibuprofen, Appl. Surf. Sci., 428 (2018) 555–565.

[26] Y. Chen, W. Chen, Q.Z. Chen, C.H. Peng, D.W. He, K.G. Zhou, Removal of ammonia-nitrogen in wastewater using a novel poly ligand exchanger-Zn(II)-loaded chelating resin, Water Sci. Technol., 79 (2019) 126–136.

[27] A. Aydin, M. Imamoglu, M. Gulfen, Separation and recovery of gold(III) from base metal ions using melamine-formaldehyde-thiourea chelating resin, J. Appl. Polym. Sci., 107 (2008) 1201–1206.

[28] H.A. Shaheen, H.M. Marwani, E.M. Soliman, Selective adsorption of gold ions from complex system using oxidized multi-walled carbon nanotubes, J. Mol. Liq., 212 (2015) 480–486.

[29] E. Ertan, M. Gulfen, Separation of gold(III) ions from copper(II) and zinc(II) ions using thiourea-formaldehyde or urea-formaldehyde chelating resins, J. Appl. Polym. Sci., 111 (2009) 2798–2805.

[30] R. Roto, Y. Yusran, A. Kuncaka, Magnetic adsorbent of $Fe_3O_4$@$SiO_2$ core-shell nanoparticles modified with thiol group for chloroauric ion adsorption, Appl. Surf. Sci., 377 (2016) 30–36.

[31] H.M. Al-Saidi, The fast recovery of gold(III) ions from aqueous solutions using raw date pits: kinetic, thermodynamic and equilibrium studies, J. Saudi Chem. Soc., 20 (2016) 615–624.
[32] K. Fujiwara, A. Ramesh, T. Maki, H. Hasegawa, K. Ueda, Adsorption of platinum(IV), palladium(II) and gold(III) from aqueous solutions onto L-lysine modified crosslinked chitosan resin, J. Hazard. Mater., 146 (2007) 39–50.
[33] M. Wojnicki, E. Rudnik, M. Luty-Blocho, K. Paclawski, K. Fitzner, Kinetic studies of gold(III) chloride complex reduction and solid phase precipitation in acidic aqueous system using dimethylamine borane as reducing agent, Hydrometallurgy, 127 (2012) 43–53.
[34] B.J. Gao, X.H. Wang, Y.Y. Zhang, Preparation of chromate anion surface-imprinted material IIP-PVI/$SiO_2$ based on polyvinylimidazole-grafted particles PVI/$SiO_2$ and its ionic recognition characteristic, Mater. Chem. Phys., 140 (2013) 478–486.
[35] M. Monier, D.A. Abdel-Latif, Fabrication of Au(III) ion-imprinted polymer based on thiol-modified chitosan, Int. J. Biol. Macromol., 105 (2017) 777–787.